

Given the apparent similarities between Ce and Mn, it can be argued that *in situ* redox chemistry must be of prime importance in contributing to surface Mn maxima.

Cerium oxidation is faster in Vineyard Sound than in the Sargasso Sea, but it is relatively less important than Ce(III) uptake. After 40 h, 70% of the ^{139}Ce uptake is the result of Ce oxidation in the Sargasso Sea at 120 m but only 30% in Vineyard Sound. Furthermore, because Ce(III) uptake occurs on a shorter timescale than Ce(III) oxidation, oxidation is relatively less important in environments where particle residence times are short. Therefore, Ce anomalies should be less pronounced in areas of high particle flux than low flux, and this is generally the case. Estuarine and coastal regions have little or no Ce anomaly, whereas oligotrophic waters have large negative Ce anomalies^{1,4,14,15}. Adsorption kinetic data obtained from radio-tracer experiments may be incorporated into non-equilibrium models of trace-element scavenging. For many elements (such as thorium, tin, scandium and zinc) this is difficult because of complex adsorption kinetics²⁰. As the Ce anomaly seems to arise from a unique process with relatively straightforward kinetics, development of a Ce scavenging model may be a useful starting point for extension to more-complicated systems. Such a model would also allow more accurate predictions of the response of the Ce anomaly to changes in oceanic redox conditions. □

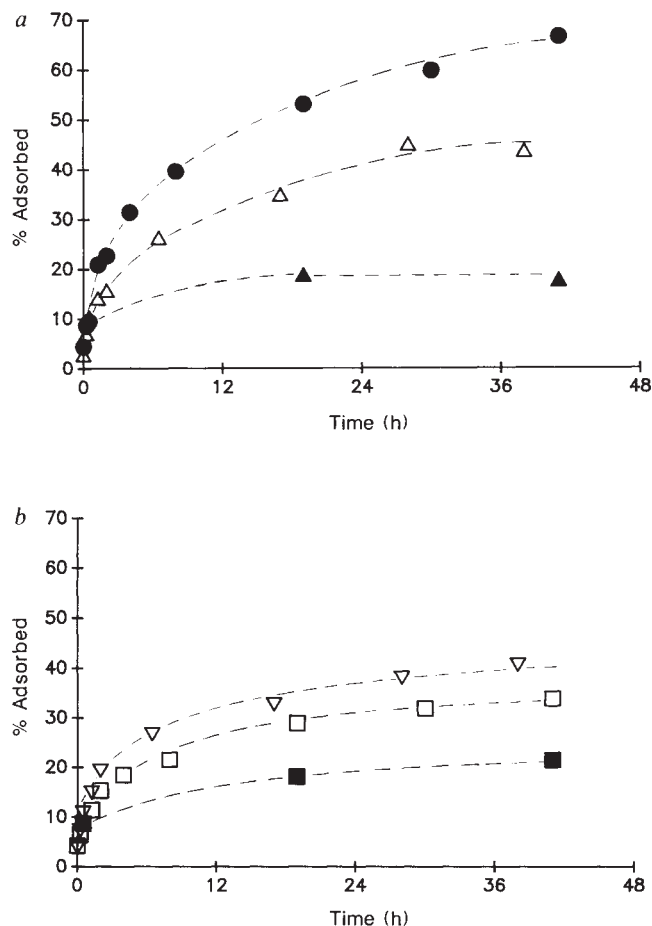


FIG. 3 Fraction of added radiotracers adsorbed on 0.2- μm -filterable particles in Vineyard Sound samples. Samples collected from a small boat in a Pyrex carboy at a location 7 km southeast of Woods Hole (10 August 1988). Samples were treated as for Sargasso samples. a, ●, ^{139}Ce ; △, ^{139}Ce + azide; ▲, ^{139}Ce + ascorbate. b, □, ^{152}Eu ; ▽, ^{152}Eu + azide; ■, ^{152}Eu + ascorbate. Absolute precision = $\pm 5\%$. Eu uptake was significantly higher in azide-treated samples than in non-treated samples. This may be the result of alteration of particulate matter by azide or may reflect real differences between samples. Differences are small relative to other differences in this figure.

Received 21 December 1989; accepted 9 April 1990.

1. Elderfield, H. *Phil. Trans. R. Soc. Lond.* **A325**, 105-126 (1988).
2. Goldberg, E. D., Koide, M., Schmitt, R. A. & Smith, R. H. *J. geophys. Res.* **68**, 4209-4217 (1963).
3. Elderfield, H. & Pagett, R. *Sci. Tot. Environ.* **49**, 175-197 (1986).
4. Sholkovitz, E. R. & Elderfield, H. *Global Biogeochem. Cycles* **2**, 157-176 (1988).
5. Murphy, K. & Dymond, J. *Nature* **307**, 444-447 (1984).
6. Elderfield, H., Hawkesworth, C. J., Greaves, M. J. & Calvert, S. E. *Geochim. cosmochim. Acta* **45**, 1231-1234 (1984).
7. Cantrell, K. J. & Byrne, R. H. *Geochim. cosmochim. Acta* **51**, 597-605 (1987).
8. Sunda, W. G. & Huntsman, S. A. *Deep Sea Res.* **35**, 1297-1317 (1988).
9. Tebo, B. M. & Emerson, S. *Biogeochem.* **2**, 149-161 (1982).
10. Turner, D. R., Whitfield, M. & Dickson, A. G. *Geochim. cosmochim. Acta* **45**, 855-882 (1981).
11. Landing, W. & Bruland, K. W. *Geochim. cosmochim. Acta* **51**, 29-43 (1987).
12. Martin, J. H. & Knauer, G. A. *Earth planet Sci. Lett.* **51**, 266-274 (1980).
13. De Baar, H. J. W., Bacon, M. P. & Brewer, P. G. *Nature* **301**, 203-204 (1983).
14. De Baar, H. J. W., Bacon, M. P., Brewer, P. G. & Bruland, K. W. *Geochim. cosmochim. Acta* **49**, 1949-1953 (1985).
15. German, C. thesis, Cambridge Univ. (1988).
16. Orians, K. J. & Bruland, K. W. *Nature* **316**, 427-429 (1984).
17. Coale, K. H. & Bruland, K. W. *Limnol. Oceanogr.* **32**, 189-200 (1987).
18. Rahn, K. A. *The Chemical Composition of Atmospheric Aerosol, Tech. Rep. 265* (Univ. of Rhode Island, 1976).
19. Schneider, B. *J. geophys. Res.* **90**, 10744-10746 (1985).
20. Jannasch, H. W., Honeyman, B. D., Balistrieri, L. S. & Murray, J. W. *Geochim. cosmochim. Acta* **52**, 567-577 (1988).

ACKNOWLEDGEMENTS. I thank E. Sholkovitz and W. Sunda for discussions. This work was supported by the NSF.

Ocean-ridge basalt compositions correlated with palaeobathymetry

M. J. Keen*, E. M. Klein† & W. G. Nelson‡

* Atlantic Geoscience Centre, Geological Survey of Canada, Bedford Institute of Oceanography, Dartmouth, Nova Scotia, Canada, B2Y 4A2

† Department of Geology, Duke University, Durham, North Carolina 27708, USA

‡ Smithsonian Institution, Washington, DC 20560, USA

KLEIN and Langmuir¹ investigated the relationships between the chemistry and water depth of eruption of zero-age mid-ocean-ridge basalts around the world. They showed that the regionally averaged values of the major-element oxides Na_2O and FeO , corrected for low-pressure fractionation, and the ratio $\text{CaO}/\text{Al}_2\text{O}_3$, correlate with their axial depths. Klein and Langmuir pointed out that the same principles should also apply to older ocean crust, where the relationships that they had established could be used as 'calibration curves', and that there was a "possibility of petrologically constraining the origins of bathymetric anomalies throughout the ocean basins"¹. Keen² showed that this can be achieved if the initial depths of eruption of older basalts are found by correcting their present depths below sea level for sediment loading and thermal subsidence. Here we show that the chemistry of basalts from older oceanic crust in the Atlantic and Indian Oceans correlates with their depth restored in this way to the original water depth at the time of eruption.

The Ocean Drilling Program's Hole 647A in the extinct mid-ocean ridge of the Labrador Sea illustrates our approach (Figs 1 and 2). Basalts were encountered at 4,561 m below sea level, beneath 699 m of sediment^{3,4}. They are typical mid-ocean-ridge basalts (MORB), 56 Myr old, but still fresh⁵. Values of Na_2O and FeO corrected for low-pressure fractionation to a common MgO value of 8 wt%, $\text{Na}_{8.0}$ and $\text{Fe}_{8.0}$ respectively, and the ratio $\text{CaO}/\text{Al}_2\text{O}_3$, have been calculated for each of the analyses⁵ that meets the criteria established by Klein and Langmuir¹ in terms of the range of acceptable values of MgO wt% (Table 1).

We found the initial depth of eruption of the basalts by 'back-tracking'⁶. Sediments have depressed the ocean crust at site 647A, and so the basalts have been 'unloaded' assuming point-wise Airy isostasy⁷, using a mean value of sediment density calculated from the set of measurements for the site³ (Table 1). The ocean crust at site 647A has also subsided thermally, and this subsidence has also been restored. We assume that the average depth at which ocean crust is formed is 2,500 m (ref. 8).

TABLE 1 Sites on mid-ocean ridges

(1)	(2)	(3)	(4)	(5)	(6)	(7)	(8)			(11)	(12)	(13)	(14)	(15)	(16)	(17)
							Restored	Unloaded	Now							
Site	Lat. (deg)	Long. (deg)	Depth (m)	Sediment (m)	Igneous section (m)	Basalt age (Ma)	Depth to basalts			Source glass rock	Na _{8.0}	Fe _{8.0}	Number of Na, Fe analyses	CaO/Al ₂ O ₃	Number of Ca/Al analyses	Refs
14	28.33 S	20.94 W	4,346	107	1.5	39	2,229	4,415	4,453	SG	—	—	—	0.740	1	20
15	30.89 S	17.98 W	3,938	141	1.4	21	2,465	4,031	4,079	SG	2.30	8.92	1	0.837	1	20
18	27.99 S	08.01 W	4,022	178	0.3	26	2,363	4,148	4,200	SG	—	—	—	0.777	1	20
19	28.54 S	23.68 W	4,685	141	4.3	51	2,284	4,783	4,826	SG	2.20	9.50	1	0.826	1	20
105	34.90 N	69.17 W	5,245	623	9	156	2,044	5,676	5,875	SG	2.06	10.45	1	0.804	1	21–24
335	37.30 N	35.20 W	3,188	454	108	13	2,244	3,506	3,642	SG	2.40	9.45	1	0.761	1	24–27
350	67.06 N	08.29 W	1,275	362	18	41	−668	1,566	1,637	DR	1.89±0.04	9.64±0.12	3	0.767±0.010	3	28
407	63.94 N	30.58 W	2,472	304	155	35.5	629	2,714	2,776	SG	1.78	10.25	1	0.817	1	24, 29
409	62.62 N	25.95 W	832	80	239	2.4	352	894	912	DG	1.63±0.20	9.17±0.09	2	0.835±0.023	2	24, 29
417D	25.11 N	68.04 W	5,482	343	366	118	2,320	5,733	5,830	SG	2.09±0.10	9.92±0.32	22	0.825±0.016	22	30, 36
418A	25.04 N	68.06 W	5,511	324	544	118	Combine 417 and 418									30, 36
558	37.77 N	37.34 W	3,754	408	154	37	1,873	4,002	4,162	SG	2.27±0.13	9.67±0.05	2	0.755±0.016	3	31
559	35.12 N	40.92 W	3,754	238	63	35	1,857	3,927	3,992	SG	2.43	9.62	1	0.725	1	31
563	33.64 N	43.77 W	3,786	365	19	35.5	1,948	4,033	4,151	SG	2.16±0.01	10.02±0.18	3	0.833±0.027	3	31
564	33.74 N	43.77 W	3,820	284	81	35.5	1,940	4,025	4,104	SG	2.17	10.06	1	0.773	1	31
647A	53.33 N	45.26 W	3,862	699	37	56	1,692	4,311	4,561	DR	1.93±0.18	11.14±0.69	9	0.828±0.033	14	3–5
765D	15.98 S	117.58 E	5,724	924	271	139	2,720	6,270	6,648	DR	2.05±0.23	9.24±1.10	10	0.805±0.030	10	32, 33
All	23.42 N	52.03 W	5,615	<100	D	47	3,216	5,615	5,615	SG	2.57	8.52	1	0.691±0.038	2	34, 35

(1) Data. Rationale: Mid-Atlantic Ridge and its satellites—a coherent body of data; older than 20 Myr so that subsidence would be significant; 335, from our initial pilot study; 765D (Indian Ocean), deep now; All, deep formerly; 350, 407 and 409, shallow now and formerly. The data shown here form the complete Smithsonian data base for Atlantic glasses older than 20 Myr, supplemented by whole-rock data and DSDP glass data for extremes in depth. No data analysed have been excluded. (6) Section drilled through igneous rocks. D, dredge haul. (7) Age: ref. 36 throughout. (8) and (9), Density: sea water, 1.03 g cm⁻³; mantle, 3.33 g cm⁻³. (11) Source: D, Deep Sea Drilling Project/Ocean Drilling Program volumes; S, Smithsonian Volcanic Glass Project Data; G, glass; R, whole rock. (12)–(16) Criteria for inclusion in Table 1 and in plots. All data: meet MgO criteria of ref. 1. Smithsonian Volcanic Glass Project Data: inclusion in that data base. Glass analyses, DSDP: 409: ref. 37, Table 3, samples 409 7 6b, 409 13 2; both glasses; K₂O mean 0.15. We observe that the average of the two totals is 97.80. Whole-rock analyses: DSDP/ODP: 350: ref. 28, p. 661, Table 3, three analyses: H₂O (total) average 1.16; K₂O average, 0.28; total average, 99.27. 647A: ref. 5, Table 1: analyses for Site 647A: total average, 99.38; K₂O average, 0.05; average H₂O + 1.38 (of eight analyses reporting). 765D: ref. 32, analyst T. Plank: Table 765-P-2, analyses with 0.0 < LOI < 0.6; these had: total average, 99.52; K₂O average, 0.50; LOI average, 0.33. LOI is loss on ignition. (12), (13) and (15), Fig. 3: correction for low-pressure fractionation: see refs 1, 2; Na_{8.0} = Na₂O + 0.373 × (MgO) − 2.98; Fe_{8.0} = FeO + 1.664 × (MgO) − 13.313. Na_{8.0} and Fe_{8.0} are calculated for samples with 5.0–8.5% MgO. CaO/Al₂O₃ are calculated for samples with >5.0% MgO. Fe_{8.0} = 2.033 × (5.233 − b_{Fe}), where b_{Fe} = Na_{8.0} − 0.19 × Fe_{8.0}. (14) and (16), Numbers of analyses: numbers of analyses available that passed screening.

After 56 Myr, crust formed at this water depth should have subsided to 5,119 m (Table 1). But the depth of the basalts at site 647A corrected for unloading (4,311 m) is 808 m less than this. Assuming that initial differences in elevation are preserved as the crust subsides overall, the initial depth of the crust at site 647A becomes 1,692 m, not 2,500 m. This value is consistent with the generally shallow crust in the Labrador Sea, attributed to the effects of a hotspot that developed about 60 Myr ago^{4,9–11}

beneath the Davis Strait to the north or beneath eastern Greenland.

At their present depth below sea level, the Na_{8.0} value for basalts from site 647A does not plot in the field defined by Klein and Langmuir¹. But the value does plot in this field after the site is restored to its initial water depth by correcting for the effects of loading and thermal subsidence (Fig. 1).

The chemistry of older basalts from the other sites that we studied in the Atlantic and Indian Oceans shows the same relationship to the initial depth as it does at site 647A (Table 1; Figs 2 and 3). Figure 3 shows that values of Na_{8.0}, CaO/Al₂O₃ and Fe_{8.0} in general fall within the fields defined by Klein and Langmuir¹ when the basalts are restored to their original water depths at the time of crustal formation. Furthermore, Fig. 3 shows that the relationship between chemistry and initial water depth at these sites holds over at least a substantial part of the range delineated by Klein and Langmuir¹, including shallow sites close to known hotspots such as Iceland¹.

Although the data for older basalts restored to initial water depths in general fall within the fields defined by Klein and Langmuir¹, there is only a weak inverse correlation between restored depth and Fe_{8.0}. This is consistent with the weaker correlation for zero-age basalts between regional averages of depth and Fe_{8.0} compared with the correlations between depth and Na_{8.0} or CaO/Al₂O₃ (refs 12 and 13). Klein and Langmuir¹² suggested that because iron abundances primarily reflect the pressure of melting, the weaker correlation for Fe_{8.0} may reflect in part the sampling of instantaneous melts from different pressures within a zone of melting. They proposed an algorithm to isolate the component of iron variation that reflects regional differences in solidus pressure and noted a good inverse correlation between this parameter (Fe_{8.0}^G) and depth for individual analyses (Fig. 3g, h). The data for individual analyses for older basalts also show a good correlation between Fe_{8.0}^G and restored depth, and fall within the field of data presented by Klein and Langmuir¹².

In an approach such as this, uncertainty may arise from several sources. First, the chemical composition of ocean basalts is often altered by interactions with sea water. We therefore used analy-

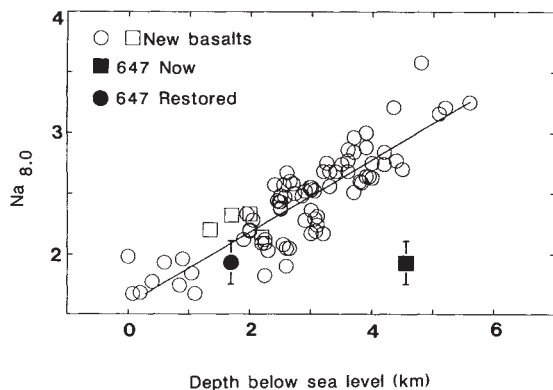


FIG. 1 The average Na_{8.0} value of the 56-Myr-old basalts from Ocean Drilling Program site 647A (Na₂O wt% corrected for low-pressure fractionation¹) plots in the field established by Klein and Langmuir¹ for zero-age axial basalts when restored to the initial water depth of site 647A (●), but not at the present depth below sea level of the basalt (■). ○, □ ('new'): ○, values for present-day ocean ridge basalts world-wide¹; □, values described by Klein and Langmuir¹ as 'anomalous' from various axial hotspot centres. ■ ('647 now'): average value of Na_{8.0} for fresh basalts from site 647A plotted at the present depth below sea level of the basalts. ● ('647 restored'): the same value plotted at the depth of the basalts restored to the initial depth at the time of formation by correcting for sediment loading and thermal subsidence (see text). Bars: one standard deviation about the mean Na_{8.0} value. Lines: linear regression on the open circles plotted solely as an aid to the eye.

ses of fresh glasses where we could, from the Smithsonian Volcanic Glass Data Base¹⁴ and the Deep Sea Drilling Project (see refs in Table 1). These have been supplemented by whole-rock analyses of fresh rocks for the three sites representing extremes in depth where glass analyses were not available (Table 1); these bulk analyses, however, may not reflect liquid compositions because of the presence of phenocrysts in some samples. We have attempted to estimate chemical variability among samples from a single site using the standard deviation about the average values at sites where more than one group of samples was available (Fig. 3, Table 1).

Uncertainty also arises in restoration to initial depth because of the corrections for sediment loading, the effects of errors in crustal age on estimates of thermal subsidence, and the assumption that initial differences in elevation at ridge crests are preserved as the crust subsides. The correction for sediment loading depends on the average density of the sediment column⁶, and this can be estimated from bulk measurements of density, the sediment thickness⁷, or the two-way reflection time at the site¹⁵. Comparisons of the three methods at the sites that we used show that this uncertainty is in the range of only tens of metres. Similarly, errors in crustal age are usually sufficiently small that we can neglect the uncertainty they cause in restoring thermal subsidence.

The assumption that initial elevations are preserved is well established for 'normal' mid-ocean ridges and for aseismic ridges⁶. It provides a clear reference for the sites used here, and independent evidence supports many of the initial depths that we have predicted. For example, the crest of the Mid-Atlantic Ridge along the flow line east of the site AII is deeper than normal at present¹⁶, and other studies indicate that sites near Iceland (such as 350, 407, 409) and sites younger than about 36 Myr near the Azores (559, 563, 564) should be shallow, as we find¹⁷. Probing the details of such depth anomalies will be interesting; for example, the original depths of sites now on swells will depend on the timing of their formation with respect to that of the swell itself.

Consequently, the correlations we see between restored initial eruption depths and major-element geochemistry—the right-

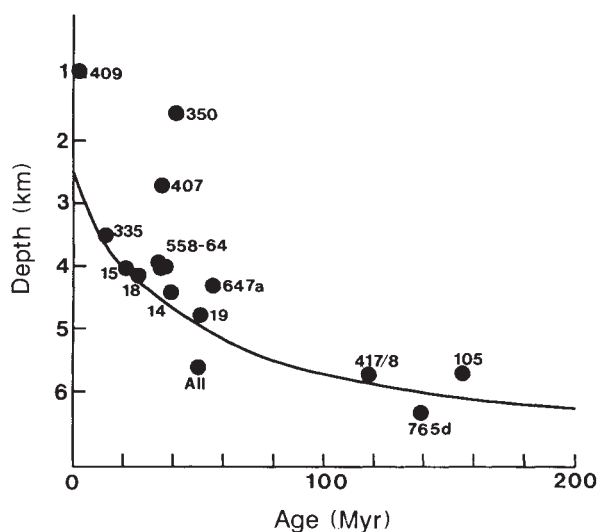


FIG. 2 The sites used in this study plotted at their unloaded depths and ages. The unloaded depth is the present depth of the basalt at a site below sea level, corrected for loading by sediments. The solid curve is the average subsidence curve for the ocean crust⁸. All locations represent Deep Sea Drilling Project or Ocean Drilling Program site numbers, except for AII—a dredge haul from the western North Atlantic³⁴. See Table 1 for locations.

hand panels of Fig. 3—lead us to suggest that our observations on basalts from older oceanic crust in the Atlantic Ocean (and from the one site in the Indian Ocean) support and extend the hypothesis of Klein and Langmuir¹ over a wide range of initial depths and age. The hypothesis seems to have survived a rather robust test.

Klein and Langmuir¹ noted a correlation between crustal thickness and basalt chemistry, and suggested that the covariations among zero-age depth, chemistry and crustal thickness result from variations in subsolidus mantle temperatures. Efforts to relate oceanic crustal thickness to other physical parameters have only rarely been successful^{18,19}. Our results indicate that

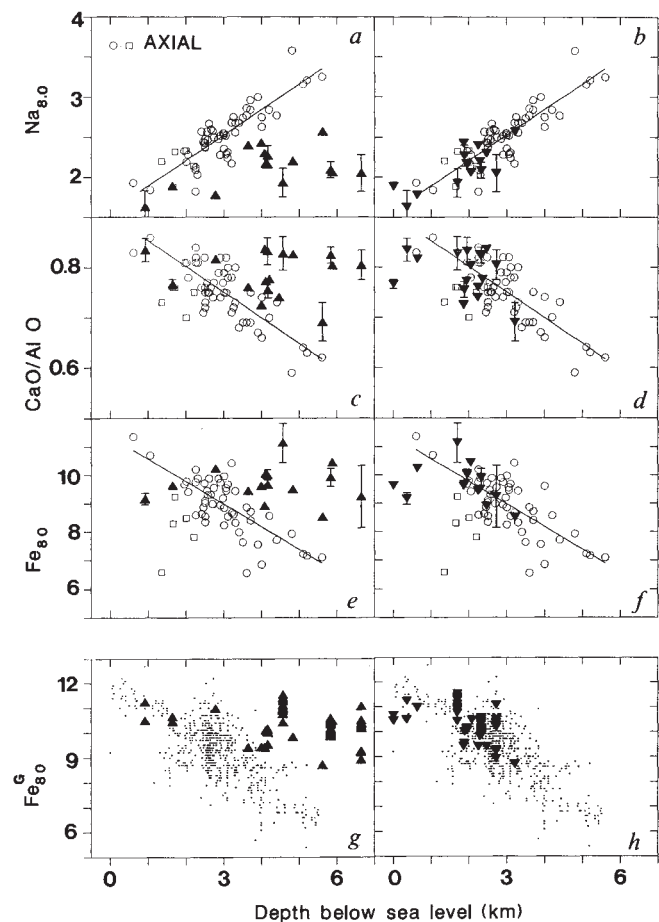


FIG. 3. The major-element geochemistry of older basalts from the mid-ocean ridges of the ocean basins correlates with the original water depth of the basalts (the depth when the basalts erupted). The variations in averaged Na_2O and FeO corrected for low-pressure fractionation ($\text{Na}_{8.0}$ and $\text{Fe}_{8.0}$), in averaged $\text{CaO}/\text{Al}_2\text{O}_3$, and in individual analyses of $\text{Fe}_{8.0}^G$ fall within the fields defined by Klein and Langmuir^{1,12} for zero-age axial basalts after restoration to their original depths. $\text{Fe}_{8.0}^G$ is the iron variation calculated to maximize the component of iron that reflects solidus pressure¹² (see text). *a, c, e, g*, $\text{Na}_{8.0}$, $\text{CaO}/\text{Al}_2\text{O}_3$, $\text{Fe}_{8.0}$, $\text{Fe}_{8.0}^G$, respectively. Values from older basalts from the oceanic ridges of the Atlantic Ocean and Indian Ocean (one site) (Table 1) with standard deviations where available, plotted at their present depths below sea level (\blacktriangle , 'present depth'). They do not fall into the fields defined by the modern axial basalts (\circ , \square , dots). *b, d, f, h*, $\text{Na}_{8.0}$, $\text{CaO}/\text{Al}_2\text{O}_3$, $\text{Fe}_{8.0}$, $\text{Fe}_{8.0}^G$, respectively. Values from older basalts from the oceanic ridges restored to their original water depths at the time of formation by correcting present basement depths for loading by sediments and for thermal subsidence (\blacktriangledown , 'restored depths'). They fall within the same fields as the zero-age axial basalts. Lines: linear regression on the open circles, plotted only as an aid to the eye comparing left and right panels. *a-f*, \circ and \square , ('axial'): regional averages of zero-age axial basalts^{1,12} (see caption to Fig. 1). *g* and *h*, dots: individual analyses of $\text{Fe}_{8.0}^G$ for zero-age axial basalts¹².

we should extend the approach that we have devised here, and explore the relationships between crustal thickness and restored initial depth. Crustal thickness may perhaps be established more reliably on older crust than on younger crust, and so we may have opened up the possibility of more fruitful investigations of the relationships between depth, crustal thickness and crustal composition than have been possible before. Klein and

Langmuir¹ also suggested that temporal variations in mantle temperatures may be explored by sampling older oceanic crust along a flow line emanating from a particular ridge segment. Our results show that the correlation between zero-age chemistry and depth can indeed be extended to older oceanic basalts, and make it attractive to seek systematic temporal variations in mantle temperature from studies of older crust. □

Received 8 January; accepted 20 March 1990.

1. Klein, E. M. & Langmuir, C. H. *J. geophys. Res.* **92**, 8089–8115 (1987).
2. Keen, M. *J. Trans. Am. geophys. Un.* **70**, 1400 (1989).
3. Srivastava, S. P. *et al. Proc. Ocean Drilling Program, Init. Rep.* **105**, 675–725 (1987).
4. Srivastava, S. P. & Arthur, M. A. *Proc. Ocean Drilling Program, Scientific Results* **105**, 989–1089 (1989).
5. Clarke, D. B., Cameron, B. I., Muecke, G. K. & Bates, J. L. *Can. J. Earth Sci.* **26**, 956–968 (1989).
6. Sclater, J. G., Meinke, L., Bennett, A. & Murphy, C. *Mem. geol. Soc. Am.* **163**, 1–19 (1985).
7. Le Douaran, S. & Parsons, B. *J. geophys. Res.* **87**, 4715–4722 (1982).
8. Parsons, B. & Sclater, J. G. *J. geophys. Res.* **82**, 803–827 (1977).
9. Hyndman, R. D. *Can. J. Earth Sci.* **10**, 637–644 (1973).
10. Keen, C. E. & Barrett, D. L. *Geophys. J. R. astr. Soc.* **30**, 253–271 (1972).
11. White, R. & McKenzie, D. *J. geophys. Res.* **94**, 7685–7730 (1989).
12. Klein, E. M. & Langmuir, C. H. *J. geophys. Res.* **94**, 4241–4252 (1989).
13. Brodholt, J. P. & Batiza, R. *J. geophys. Res.* **94**, 4231–4239 (1989).
14. Nelson, W. G. & O'Hearn, T. in *The Geology of North America, Volume M, The Western North Atlantic Region* (eds Vogt, P. R. & Tucholke, B. E.) 117–136 (Geol. Soc. Am., Boulder, 1986).
15. Crough, S. T. *J. geophys. Res.* **88**, 6449–6454 (1983).
16. Sclater, J. G., Lawver, L. A. & Parsons, B. *J. geophys. Res.* **80**, 1031–1052 (1975).
17. Sclater, J. G., Hellinger, S. & Tapscoff, C. *J. Geol.* **85**, 509–552 (1977).
18. Purdy, G. M. & Ewing, J. in *The Geology of North America, Volume M, The Western North Atlantic Region* (eds Vogt, P. R. & Tucholke, B. E.) 313–330 (Geol. Soc. Am., Boulder, 1986).
19. Reid, I. & Jackson, H. R. *Mar. geophys. Res.* **5**, 165–172 (1981).
20. Maxwell, A. E. *et al. Init. Rep. DSDP Leg 3* (1970).
21. Hollister, C. D. *et al. Init. Rep. DSDP Leg 11* (1972).

22. Vogt, P. R. & Tucholke, B. E. (eds) *The Geology of North America, Volume M, The Western North Atlantic Region* (Geol. Soc. Am., Boulder, 1986).
23. Sclater, J. G. & Wixon, L. in *The Geology of North America, Volume M, The Western North Atlantic Region* (eds Vogt, P. R. & Tucholke, B. E.) 257–270 (Geol. Soc. Am., Boulder, 1986).
24. Bryan, W. B. & Frey, F. A. in *The Geology of North America, Volume M, The Western North Atlantic Region* (eds Vogt, P. R. & Tucholke, B. E.) 271–296 (Geol. Soc. Am., Boulder, 1986).
25. Aumento, F. *et al. Init. Rep. DSDP Leg 37* (1977).
26. Howe, R. C. *Init. Rep. DSDP Leg 37*, 909–916 (1977).
27. Miles, G. A. *Init. Rep. DSDP Leg 37*, 929–962 (1977).
28. Talwani, M., Udintsev, G. *et al. Init. Rep. DSDP Leg 38* (1976).
29. Luyendyk, B. P. *et al. Init. Rep. DSDP Leg 49* (1978).
30. Donnelly, T. *Init. Rep. DSDP Legs 51–53* (1979).
31. Bougault, H. *et al. Init. Rep. DSDP Leg 82* (1985).
32. Ludden, J. *et al. Proc. Ocean Drilling Program Init. Rep.* **123**, 230–289 (1990).
33. *JOIDES J.* **15**(1), 3–7 (1989).
34. Ludden, J. N. & Thompson, G. *Earth planet. Sci. Lett.* **43**, 85–92 (1979).
35. Klitgord, K. & Schouten, H. in *The Geology of North America, Volume M, The Western North Atlantic Region* (eds Vogt, P. R. & Tucholke, B. E.) 351–378 (Geol. Soc. Am., Boulder, 1986).
36. Kent, D. V. & Gradstein, F. M. in *The Geology of North America, Volume M, The Western North Atlantic Region* (eds Vogt, P. R. & Tucholke, B. E.) 45–50 (Geol. Soc. Am., Boulder, 1986).
37. Wood, D. A. *et al. Init. Rep. DSDP Leg 49*, 597–655 (1978).

ACKNOWLEDGEMENTS. We thank C. E. Keen, D. J. W. Piper, D. B. Clarke, F. Gradstein, R. Courtney, R. D. Hyndman, T. Plank, C. H. Langmuir, J. Cann, S. Srivastava, R. White, G. Thompson and J. Bogen for suggestions, staff of the Ocean Drilling Program Office and T. O'Hearn for assistance with electron microprobe analyses of glasses.

Seismic quiescence at Parkfield: an independent indication of an imminent earthquake

M. Wyss*, P. Bodin* & R. E. Habermann†

* Cooperative Institute for Research in Environmental Science/Department of Geology, University of Colorado, Boulder, Colorado 80309, USA

† National Geophysical Data Center of NOAA, Boulder, Colorado 80303, USA

THE Parkfield segment of the San Andreas fault midway between San Francisco and Los Angeles has experienced six moderate-sized earthquakes since 1850, with an average recurrence time of about 22 years. Based on this regular behaviour, and the occurrence of the most recent earthquake in 1966, a shock of local magnitude $M_L = 5.7$ is expected to occur by 1993^{1,2}. Here we suggest that a current lack of small earthquakes on this segment could be a precursory anomaly to the next characteristic Parkfield earthquake. Only four earthquakes of $M \geq 2.5$ have occurred on the segment since January 1986, whereas twenty would have been expected, extrapolating from the mean background rate. Comparison with other cases of precursory quiescence suggests that the $M = 5.7$ earthquake should occur in the next two years, rupturing the same 35-km fault segment that ruptured in 1966³.

Seismic quiescence is a phenomenon that has been used successfully to predict moderate and large earthquakes^{4–6}. Seismicity consists of two parts: events that depend on each other (clusters) and independent events. After removing the clusters from the data⁷, the remaining seismicity (background) shows a remarkably constant rate over many years. Against this constant rate a decrease by about a factor of two (seismic quiescence) that lasts for approximately a year or more is an unusual occurrence and is often followed by a mainshock⁸. The quiescence is thought to signal a change in the physical process governing the production of small earthquakes in the rupture volume.

Usually the quiescence outlines the mainshock rupture volume and affects all magnitude bands^{4–6,8–11} but it has been proposed that in some cases the rate of small-magnitude earthquakes remains constant^{12,13}.

An example of precursory seismic quiescence is shown in Fig. 1a. The Stone Canyon case was used as a basis for estimating what to expect in the Parkfield area because it occurred on the San Andreas fault about 80 km northwest of Parkfield and comes from a similar tectonic environment.

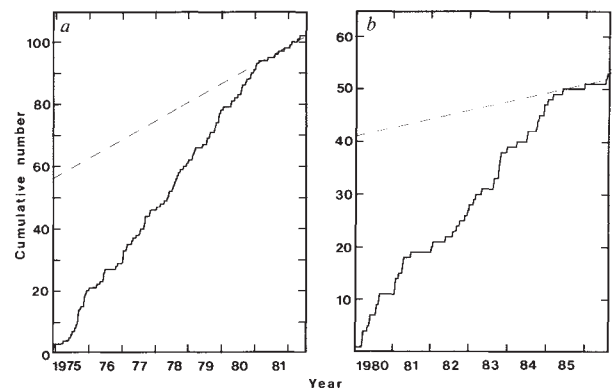


FIG. 1 Applicability of the quiescence hypothesis to the Parkfield segment of the San Andreas fault, tested by comparing the patterns of seismicity rate in the source volumes of mainshocks at a, Stone Canyon and b, Parkfield. The mainshocks ($M = 5$ at Stone Canyon, $M = 3.6$ at Parkfield) occurred at the time of the right end of the plots of cumulative seismicity (all shocks $M > 1.8$ at Stone Canyon and $M > 0.9$ at Parkfield) and quiescence started 1.5 years before the mainshocks. The slope of these curves is the mean seismicity rate. The dashed lines extrapolate the anomalously low precursory rate back in time for comparison with the observed background rate. The similarity of the pattern strongly suggests that the quiescence hypothesis should be as applicable at Parkfield as at Stone Canyon, where a successful prediction was made⁴.